Proceedings of ISABE 2015

ISABE-2015-20259

Feasibility of Self Powered Actuation for Flow, Separation and Vibration Control

Dillon Bak[1]
University of Notre Dame
Notre Dame, IN, USA

Alain Izadnegahdar[2]
SAIC/NASA GRC
Cleveland, OH, USA

Vikram Shyam[3]
NASA Glenn Research Center
Cleveland, OH, USA

[1] NASA INSPIRE high school intern at NASA GRC
[2] Senior electrical engineer, SAIC/NASA GRC
[3] Research Aerospace Engineer, NASA GRC, contact author

ABSTRACT

A gas turbine engine is anywhere from 40-50% efficient with a large amount of waste heat production. The primary focus of this work was to evaluate the feasibility of harvesting energy from sections of an imaginary but representative gas turbine engine that has large thermal gradients using thermoelectric generators (TEGs) and using the harvested energy locally for flow control using either plasma actuators or piezoelectric actuators. This work is a summary of a two- year NASA Center Innovation Fund from 2010 to 2012. The trade-off between thermoelectric harvesting and blade surface temperature was studied to ensure that blade durability is not adversely impacted by embedding a low thermal conductivity TEG. Calculations show that at least 2-3 Watts can be harvested per blade depending on flow conditions and on the thermoelectric material chosen while maintaining metal temperatures below critical limits. BiTe and SiGe were considered as TEG materials although higher ZT materials are now in development. A circuit to convert the DC power output of the TEG to AC input for plasma actuation was fabricated and tested. Several novel plasma actuator configurations were also tested.

NOMENCLATURE

R	thermal resistance
L	thickness
k	thermal conductivity
A	area
T	temperature
h	heat transfer coefficient
V	Volts
K	Kelvin
Z	figure of merit for thermoelectric
σ	electrical conductivity
S	Seebeck Coefficient
TEG	Thermoelectric Generator
ή	efficiency
P	Power extracted by TEG
Q	Power available

Subscripts

C	refers to the air used for cooling
H	hot gas
MO	outer surface of the blade
MI	inner surface of the blade
HJ	hot junction interface between the TEG and blade
m	metal
t	TEG (Thermoelectric Generator)

TEG Thermoelectric Generator

INTRODUCTION

Gas turbine engines operate on the Brayton cycle and produce thrust by combusting a fuel to convert its chemical energy into the mechanical energy of a shaft that drives a fan and compressor. To burn efficiently in the combustor, air entering the engine inlet is compressed to a high pressure (the higher the compression, the more efficient the combustion process.) The fluid exiting the combustor can reach temperatures well in excess of the component thermal limits in the high pressure turbine (HPT) section. A typical turbofan engine is shown in Figure 1 along with temperatures at various locations in the gas path. The temperatures shown correspond to a high bypass ratio engine (BPR = 10) with Overall Pressure Ratio (OPR) of 55 operating at cruise (Mach 0.85 at 35,000 ft). High operating pressure ratios as well as increased turbine inlet total temperatures are expected to be the hallmarks of NASA's N+3 engines. In order to cool the surfaces of components in the HPT, part of the air from the compressor is bled away and fed through internal passages to the HPT where the relatively cooler fluid is injected through discrete holes onto the surface of the hot components. Figure 2 shows a typical turbine vane with cooling holes. This cooling fluid is deprived of passage through the combustor and moreover, when fed into the rotor, has work done on it by the rotor instead of being used to turn the HPT blades. It is thus a goal of turbomachinery research to minimize turbine cooling air requirements while simultaneously maintaining the blade surface temperatures sufficiently below their critical limits to ensure turbine durability.

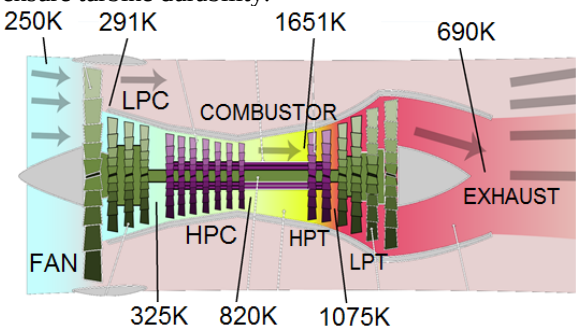

Figure 1 Cross section of a turbofan engine with representative temperatures obtained from NPSS [1] at cruise (Mach 0.85, 35k ft) for a high bypass ratio engine.

Turbomachinery is utilized for power generation, aviation and several other applications where an efficient source of mechanical energy is required. As the number of gas turbines in the world increases and as fossil fuels are becoming scarcer it is necessary to

Figure 2. Turbine vanes with cooling holes

find methods to harness all the energy available as efficiently as possible. This can be achieved by recovering waste heat and vibrational energy through energy conversion devices such as thermoelectric generators and piezoelectric harvesters respectively. TEGs make use of the Seebeck effect - if two dissimilar metals are connected in such a way that they form a circuit, and if the junctions of those two metals are held at different temperatures, an electric potential is generated between the hot and cold junctions. Looking at Figure 1, it is clear that several locations exist in a turbofan engine to harvest waste heat. Heat is lost radially through conduction in the casing walls and exhaust nozzle. Energy harvested from this temperature difference can be stored in a capacitor or battery as part of a hybrid electric engine system. Large temperature differences (~800K) also exist between the blade outer surfaces (air that's been through combustion) and their internal surfaces (exposed to cooling air.) This heat transfer is not considered waste heat because the cooling air is returned to the main flow path and turns downstream blade rows. The benefit then of harvesting energy from the temperature difference across the thickness of a turbine blade is a local power source for active flow control, actuation or sensors.

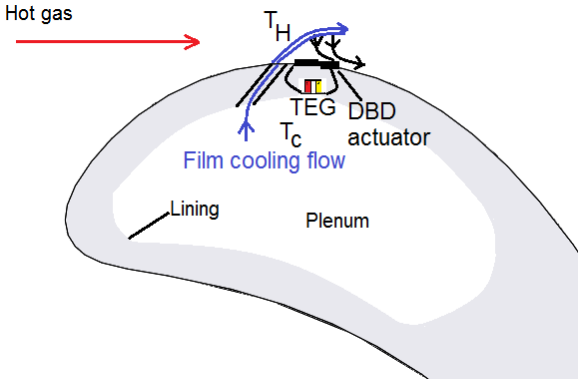

Figure 1 Self-powered DBD actuator system showing control of film cooling jet using a DBD actuator powered by energy harvested form an

embedded TEG.

CONCEPT

The concept proposed in this study (Figure 3) is to use the temperature difference across the thickness of turbine blades to generate power for local actuation. Specifically, TEGs are to be mounted in the plenum of the turbine blades to simultaneously generate power and increase the heat transfer coefficient within the plenum. In Figure 3, TH is the hot gas temperature (approximately 1650K) and TC is the coolant temperature (approximately 820K). The blade thickness is t1 and the thickness of the TEG modules is t2.

Figure 4 shows a schematic of a TEG (adapted from Wikimedia Commons [2]). The P-N junctions look very similar to the fin structure of Figure 5 that could be used to line the inner surface of the plenum to simultaneously act as fins or grooves. The purpose of the grooves or turbulators is to increase the heat transfer coefficient within the blade plenum. This draws more heat into the plenum and the heat is carried away by the coolant. This in turn reduces the amount of film cooling that is required and reduces aerodynamic mixing losses (coolant-hot gas mixing.)

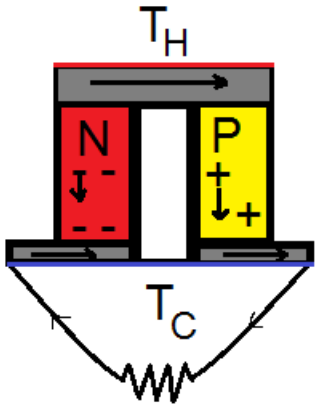

Figure 2. Schematic of a TEG.

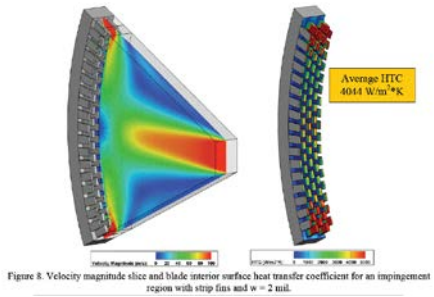

Figure 5. Micro grooves and fins in the plenum [6].

TEG efficiency of a material is characterized by a nondimensional figure of merit [3, 4, 5], $Z\bar{T} = \frac{eS^2T}{k}$, where e is the electrical conductivity, k is the thermal conductivity and S is the Seebeck coefficient that is a function of temperature. Thus, high electrical conductance and low thermal conductivity yields the best figure of merit. Most modern TEGs have figures of merit of approximately 1. A large temperature difference across the junctions leads to higher energy output. Due to their low thermal conductivity, integrating TEGs into blades would result in blocking a path for heat to flow from the surface of the blade to the coolant. Therefore, increasing the heat transfer coefficient of the coolant flow using fins, turbulators or microchannels [6] would help alleviate this problem.

Once the power is available, actuation devices can be placed locally to control flow. These could include Dielectric Barrier Discharge (DBD) plasma actuators [7], piezoelectric actuators [8] or magnetic actuators. On the scale of an aircraft jet engine turbine blade, these actuators require only a few Watts to operate. This energy is easily recovered from the heat in the turbine section of the engine. The plasma actuators can be used to energize the boundary layer by pulsing at various frequencies to prevent separation. They can also be used to add coherent structures to the flow by placing the plasma strip parallel to the flow or using tailored electrode shapes. This creates vortical structures that migrate downstream. These can be steady or unsteady depending upon the input signal. The type and magnitude of flow control achievable through plasma is dependent on the shape of the actuator and on the material selected for the dielectric. Plasma actuators have also been used to control shock boundary layer interaction by pulsing them at specific frequencies.

Piezoelectric actuators could serve 2 purposes. First, similar to plasma actuators, they could introduce appropriate frequency content into the flow and thus delay or prevent separation. Dolphin skin has been shown to control transition through compliance by formation of waves to destructively interfere with Tollmien-Schlichting waves [9]. Second, more direct control of the mean flow can also be achieved using larger amplitude deflection of the piezoelectric devices and this could be useful to maintain operability at off-design conditions.

Figure 3 shows an example of what a self-contained actuation system for a turbine vane or blade might look like for a film cooling application where the

wall jet created by a DBD plasma actuator is used to keep the coolant attached to the surface at high blowing ratios. For low pressure turbine or power turbine blades, separation control could be achieved with a similar setup.

Analysis of TEG power output

In this section an idealized model of the turbine vane is considered to provide guidance for TEG integration into vanes or blades. A well-known electrical circuit analogy was utilized to determine the maximum power that can be extracted by integrating TEGs into a turbine blade. Figure 6 shows the thermal circuit used. It assumes that a layer of TEG is embedded in the inner lining of the turbine blade (as shown in Figure 3). The percent area of the plenum used for harvesting and the thickness of the TEG modules were changed as well as the material properties and heat transfer coefficient in the plenum. Here, $R_{metal} = \frac{L}{kA}$ is the thermal resistance of each section of material with k the thermal conductivity of the material, L its thickness, and A its area (along the surface). The thermal resistance of coolant air is $R_C = 1/h_C A$, and the thermal resistance of the hot gas is $R_H = 1/h_H A$ where h_C is the local heat transfer coefficient of the coolant in the plenum and h_G is the heat transfer coefficient of the hot gas on the outer blade surface.

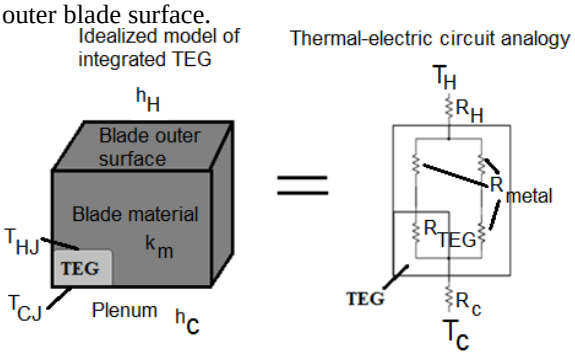

Figure 6. Left - section of blade with TEG embedded. Right - thermal circuit for TEG embedded in blade.

The net thermal resistance for this case is calculated and used to compute the heat flux through the blade, $Q = \frac{T_H - T_C}{R_{net}}$. Once the heat flux through the blade is known, the temperatures at the blade outer surface, T_{MO}, plenum lining, T_{MI}, and at the hot and cold junctions of the TEG, T_{HJ}, T_{CJ} respectively, were calculated. Note that for this case, $T_{CJ} = T_{MI}$ since the TEG cold junction coincides with the plenum lining.

To find the power that can be generated by the TEG, the Seebeck coefficient and electrical conductivity of the material must be known. In this study Bismuth Telluride (Bi_2Te_3) and Silicon Germanium (SiGe) were considered. BiTe is a material often used in TEGs at room temperature due to its superior figure of merit but is unsuitable for use at engine temperatures due to its low melting point. SiGe is another material often used in TEGs (Radioisotope Thermoelectric Generators or RTGs) for in-space power applications. SiGe is capable of withstanding higher temperatures [11] with a melting point of approximately 1600K but it is still not widely available for use. SiGe is also resistant to oxidation. The electrical conductivity, *e* and the Seebeck coefficient, S of BiTe are respectively, 110000 (S.m)/m^2 and 1.00E-4 V/K [3]. For SiGe *e* is 50000 S/m and S is 300 μV/K [12]. The thermal conductivity, k of SiGe remains fairly constant with temperature and is approximately 3 W/mK [12]. The average TEG temperature is $\bar{T} = \frac{T_H + T_C}{2}$. The nondimensional figure of merit, $Z\bar{T} = \frac{eS^2T}{k}$ is then calculated. For SiGe, ZT is approximately 1 [12] for high temperatures (>1200K). TEG efficiency is calculated using the figure of merit as $\acute{\eta} = \frac{\Delta T}{T_h} \frac{\sqrt{1+Z\bar{T}}-1}{\sqrt{1+Z\bar{T}}+T_c/T_h}$ [3]. Now, with the efficiency found, electric power can be solved for using the equation P=ή*Q [3].

A compact low power plasma generator

Once we know that local power from a thermoelectric device or a solar cell or a piezoelectric generator is available, an appropriate circuit is required to convert the low voltage DC power to high voltage AC or DC that may be required for actuation. Figure 7 shows a simplified diagram of the circuit that was fabricated to operate a plasma actuator. Figure 8 shows components of the miniature circuit that were tested in NASA's SW6 wind tunnel facility.

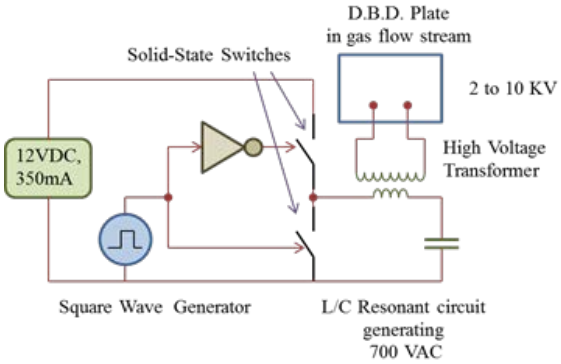

Figure 7. Circuit diagram for miniature power supply for plasma actuator.

Figure 9 shows plasma actuators being tested in the wind tunnel, powered by the miniature power

conversion circuit. The TEG was simulated using a power supply. The focus of this paper is not on plasma actuation so only Figure 10 is shown with absolute velocity contours resulting from the V-shaped actuator testing in the SW-6 wind tunnel.

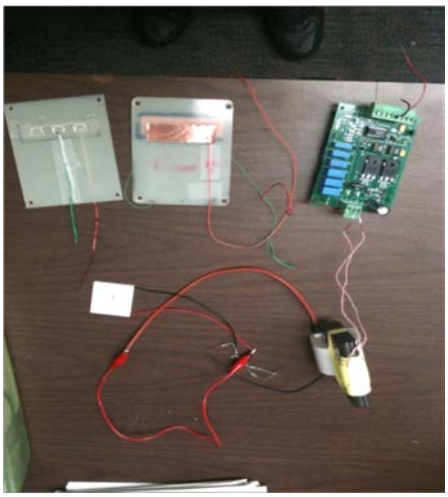

Figure 8. Components of preliminary miniature circuit.

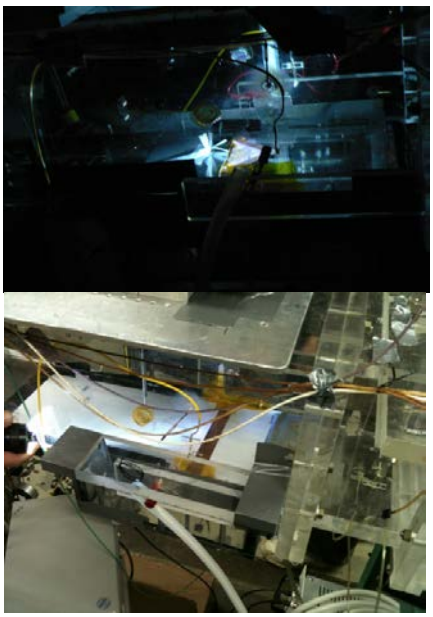

Figure 9. Plasma actuators tested using miniature circuit at 6kV. Top - Strips of paper blown by plasma 'wind' in SW-6 wind tunnel, flow from right to left. Bottom - Linear electrode plasma test plate in wind tunnel.

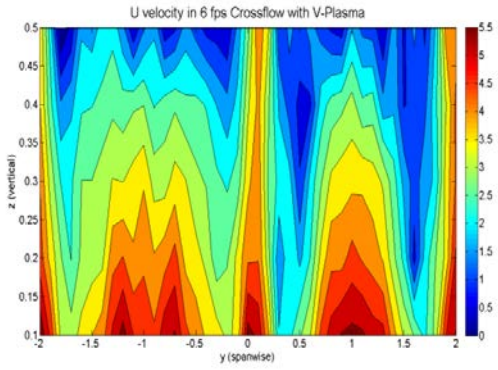

Figure 10. Contours of absolute velocity looking downstream of V-shaped actuator. Center of actuator is at y = 0. Z is vertical height above tunnel floor (z = 0.) Flow is into the figure (x-axis).

RESULTS

TEG power extraction

Due to the variation of power, P with ΔT_{43} and TEG efficiency, a corrected power, $\bar{P} = \frac{P/A}{\dot{\eta}.\Delta T_{43}}$ is presented that allows the power at various T_4 and T_3 values as well as for available blade surface area and TEG efficiency to collapse onto a single line. This is shown in figure 10 below for 3 different values of T_4. For this example, A is chosen to be 1 sq. in. (0.000645 m^2.) Other assumed parameters are shown in the figure. The heat transfer coefficients on the blade surfaces (hot gas side and plenum) are both chosen to be 1000W/m^2K. The use of corrected power allows us to look at variations of heat transfer coefficient and thermal conductivity without worrying about specific cycle temperatures.

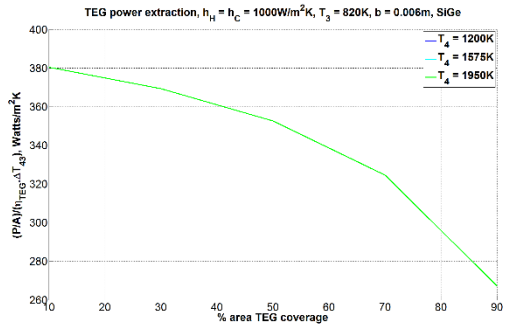

Figure 11. TEG corrected power as a function of % plenum surface area used for heat extraction.

The corresponding plot of power in Watts is shown in Figure 11. Here, it is clear that as the hot gas temperature, T_4 increases, the power extracted by the TEG increases due to a greater temperature difference existing between the TEG hot junction and

the TEG cold junction. The plenum temperature T_3 is held constant. Due to the low heat transfer coefficient in the plenum chosen for this example, the % area over which the TEG is applied in the plenum does not strongly effect the power extraction at lower temperature. Note that the corrected power decreases with increased TEG area coverage. This is because the driving temperature difference across the TEG increases due to the low thermal conductivity of the TEG. The power extracted does not increase proportionally and results in a declining power output as ΔT_{43} increases.

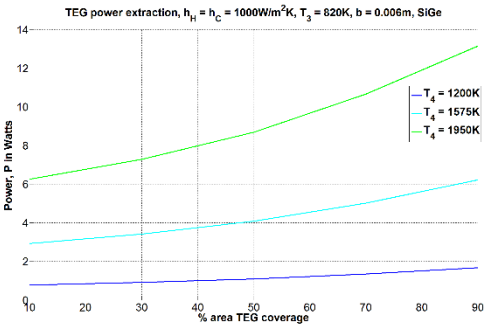

Figure 12. Power output by TEG for various hot gas temperatures as a function of % plenum surface area used for heat extraction.

Similarly, nondimensional metal temperatures, θ, are presented such that $\theta = 1 - \frac{T_4 - T}{T_4 - T_3}$, where T is the temperature to be nondimensionalized. Thus, θ = 0 corresponds to T_3 and θ = 1 corresponds to T_4. Note that the melting point of SiGe is 1600K. Assuming T_4 = 1650K and T_3 = 820K, this corresponds to θ_{limit} = 0.9398. For T_4 = 1950K, θ_{limit} = 0.69. The nondimensional hot junction temperature, θ_{HJ} must remain below this value.

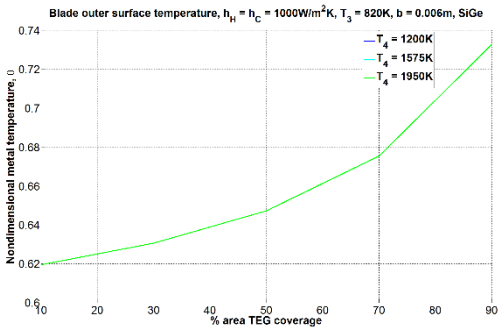

Figure 13. Blade outer surface nondimensional temperature as a function of % plenum surface area used for heat extraction.

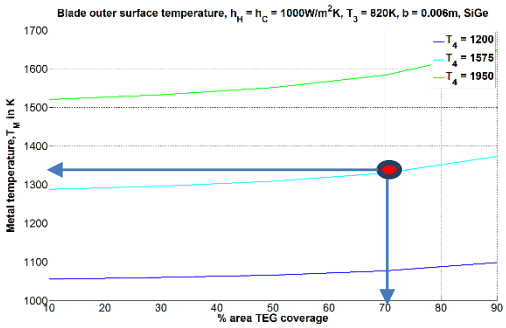

Figure 14. Blade outer surface temperature as a function of % plenum surface area used for heat extraction.

We have assumed that there is no film cooling here. Therefore, the metal temperature T_{MO} must remain below the blade material critical limit. If film cooling is present, a correction can be made to the metal temperature that allows the metal temperature to exceed the material limit based on the cooling effectiveness. For the sake of this example, let us assume a blade critical temperature of 1350K (~2000°F). Let us consider a hot gas temperature, T_4 = 1575K (2375°F). Based on Figure 14, we may not use more than 70% of the plenum surface for TEG power extraction. This is shown by the red circle in figure 14. Moving to Figure 12, this gives us approximately 5W of power.

Figure 15 shows the TEG hot junction temperature as a function of % area of the plenum lining that is used for TEG integration. At 70% TEG coverage, the hot junction temperature is approximately 1250K for T_4 = 1575K.

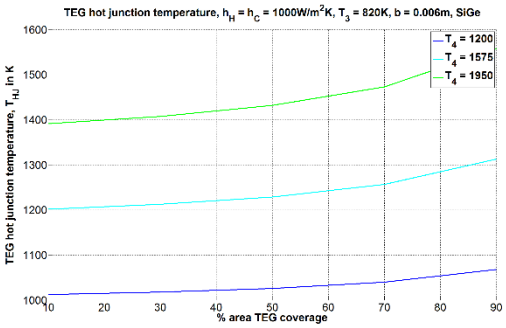

Figure 15. TEG hot junction temperature as a function of % plenum surface area used for heat extraction.

We now consider some realistic parameters and determine whether sufficient power may be extracted from a turbine blade for on-board power for actuation. We must also examine the metal temperature and hot junction temperature at take-off

condition to ensure we do not exceed material limits at take-off even though actuation may not be used (or useful) at take-off. At take-off, T_4 and T_3 are 1850K and 950K respectively from the NPSS cycle analysis.

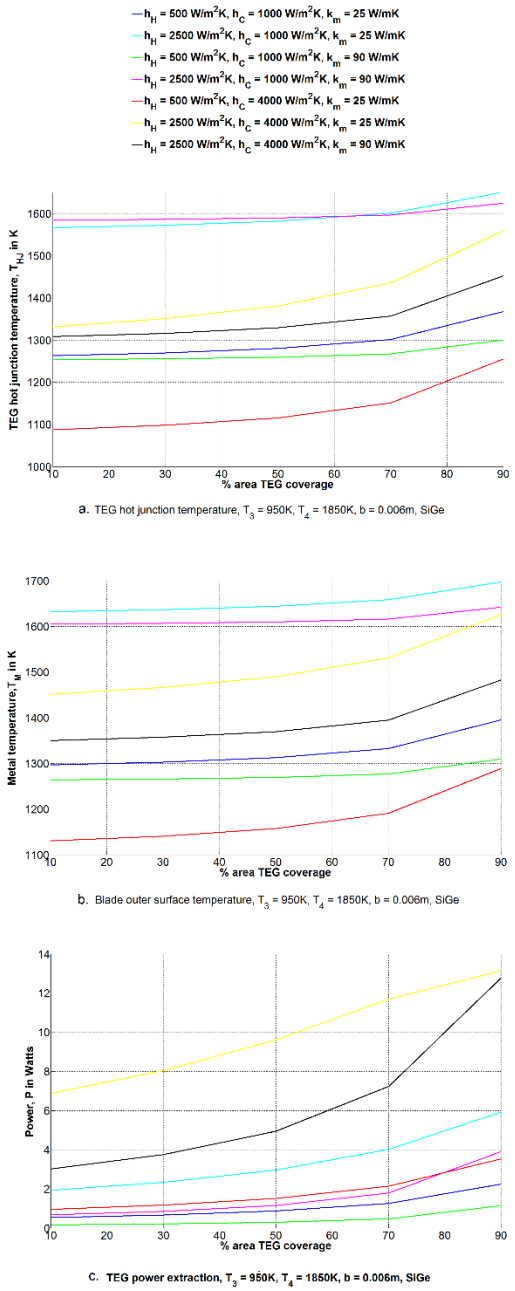

Figure 16. TEG integration into turbine vane/blade at take-off conditions. a. Hot junction temperature, T_{HJ} (must be less than 1600K) b. Blade surface temperature, T_{MO} (must be less than 1400K) and c. TEG power output, P.

As before the TEG is considered to be SiGe. The blade thickness is taken to be 0.006m (~0.23in). Usable plenum surface area is taken as .000322m^2 (0.5sq. in.) to account for unusable area due to cooling holes. It is assumed that the TEG thickness is 50% of the blade thickness. The 2 values of hot gas heat transfer coefficient, h_H considered correspond to 2 extreme cases – 500 W/m^{2}K (trailing edge regions, no film cooling) and 2500 W/m^{2}K (leading edge of vane/blade). Similarly, for the plenum, h_C = 1000 W/m^{2}K and h_C = 4000 W/m^{2}K are considered corresponding to simple ribs and microchannels respectively. Thermal conductivities of 25 W/mK and 90 W/mK are chosen to represent two hypothetical turbine blade materials (for example, single crystal superalloys and conventionally cast superalloys). The curves asymptote to the values they would have were there no TEGs as the % area decreases to 0. The gentle rise of the metal temperature for a given heat transfer coefficient and blade material below 70% TEG coverage indicates that there is a tradeoff that can be made between TEG power extraction and technology in the plenum to increase heat transfer coefficient. Higher hot gas heat transfer coefficient clearly has a negative impact on temperature and requires much higher internal heat transfer coefficient to compensate for TEGs. Note that if film cooling were present with an average film effectiveness of 0.2-0.25 for example, the effective hot gas temperature would drop to approximately 1650K and this would provide another knob to play with. If plasma actuation is able to keep a film cooling jet attached and increase effectiveness by 0.1 for example, the metal temperature would be cooler by approximately 100K. Based on Figure 16, the black line has a relatively steep increase in power output with % TEG area with a moderate temperature rise. Comparing the pink line and the black line (h_H = 2500 W/m^{2}K, h_C = 4000 W/m^{2}K and k_m = 90 W/mK),, one can see that the effect of higher plenum heat transfer coefficient (black line) is to reduce drastically the TEG cold junction temperature relative to the hot junction temperature. This keeps the power output high. For the pink line (h_H = 2500 W/m^{2}K, h_C = 1000 W/m^{2}K and k_m = 90 W/mK), low heat transfer to the plenum keeps the cold junction temperature high and results in minimal power output. The cyan line (h_H = 2500 W/m^{2}K, h_C = 1000 W/m^{2}K and k_m = 25 W/mK) and the yellow line (h_H = 2500 W/m^{2}K, h_C = 4000 W/m^{2}K and k_m = 25 W/mK) show a similar relationship with the yellow line generating 3 times more power. The only difference between the black line and the yellow line is the thermal conductivity of the blade. The higher the thermal conductivity, the smaller the temperature difference across the TEG.

Conversely, the blade surface temperature is much higher for low thermal conductivity materials. Based on Figure 16, at take-off, blades with thermal conductivity of 90W/mK could generate anywhere from 3-12W depending on blade critical temperature. Similarly, blades with thermal conductivity of 25W/mK can generate between 6-12W.

Figure 17 shows power output for cruise conditions. Blades with thermal conductivity of 90W/mK could generate anywhere from 2-12W depending on blade critical temperature. Similarly, blades with thermal conductivity of 25W/mK can generate between 6-18W.

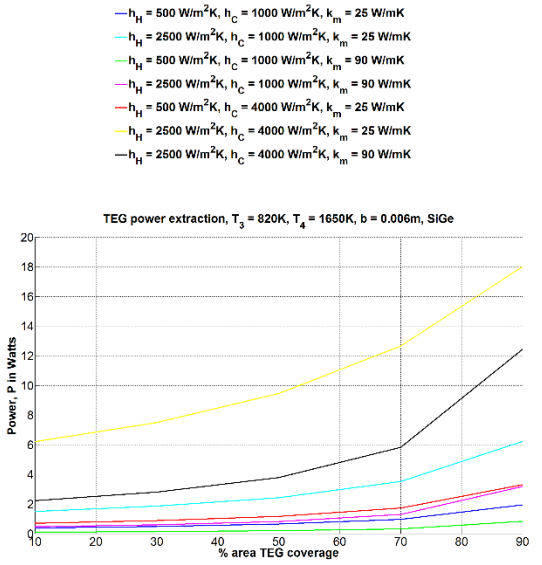

Figure 17. TEG integration into turbine vane/blade at cruise conditions showing TEG power output, P.

CONCLUSION

This study shows that with existing conditions it may be possible to supply power to an on-board flow control device such as a piezoelectric or plasma actuator. Two to three Watts alone is enough to power some devices. With the possibility of advancement in micro channel cooling, the power produced would assuredly be sufficient to run such devices.

ACKNOWLEDGEMENTS

This work was funded under 2 separate NASA Center Innovation Funds from 2010 – 2012. The authors would like to thank Dr. David Ashpis, Mr. Douglas Thurman and Mr. Phillip Poinsatte for their help with testing the V-shaped plasma actuator in NASA's SW-6 wind tunnel.

REFERENCES

1. Scott Jones, Personal communications, September 2014.

2. Wikemedia Commons

3. T. M. Tritt and M. A. Subramanian, "Thermoelectric Materials, Phenomena, and Applications: A Bird's Eye View," Mat. Rev. Soc. Bull. 31, 188 (2006).

4. Wang, X. W., Lee, H., Lan, Y. C., Zhu, G. H., Joshi, G., Wang, D. Z., Yang, J., Muto, A. J., Tang, M. Y., Latsky, J., Song, S., Dresselhaus, M. S., Chen, G., and Ren, Z.F. "Enhanced thermoelectric figure of merit in nanostructured n-type silicon germanium bulk alloy" APL_2093_20193121_202008, 14 November 2008.

5. Snyder, G. Jeffery. "Small Thermoelectric Generators" The Electrochemical Society Interface, Fall 2008.

6. Justin Jacobs, Joe Tripp, David Underwood and Corinne Lengsfeld, "Optimization of Micro-Textured Surfaces for Turbine Vane Impingement Cooling," Paper No. GT2013-94727, pp. V03AT12A024; 8 pages doi:10.1115/GT2013-9472

7. Thomas C. Corke, C. Lon Enloe, and Stephen P.Wilkinson, "Dielectric Barrier Discharge Plasma Actuators for Flow Control", Annual Review of Fluid Mechanics, Vol. 42: 505-529 (Volume publication date 2010).

8. A. Seifert, S. Eliahu, D. Greenblatt, and I. Wygnanski. "Use of Piezoelectric Actuators for Airfoil Separation Control", AIAA Journal, Vol. 36, No. 8 (1998), pp. 1535-1537. doi: 10.2514/2.549.

9. Andreas Pätzold, Inken Peltzer, Wolfgang Nitsche, "Learning from Dolphin Skin – Active Transition Delay by Distributed Surface Actuation", Book chapter from Nature-Inspired Fluid Mechanics, Notes on Numerical Fluid Mechanics and Multidisciplinary Design Volume 119, 2012, pp 179-192.

10. Narayanaswamy, Venkateswaran, Raja, Laxminarayan L. and Clemens, Noel T., "Control of unsteadiness of a shock

wave/turbulent boundary layer interaction by using a pulsed-plasma-jet actuator", Physics of Fluids, 24, 076101 (2012), DOI:http://dx.doi.org/10.1063/1.4731292.

11. L.D. Hicks, M.S. Dresselhaus, Phys. Rev. B 47, 12727, 1993.

12. Tayebi, L.; Zamanipour, Z.; Mozafari, M.; Norouzzadeh, P.; Krasinski, J.S.; Ede, K.F.; Vashaee, Daryoosh, "Thermal and Thermoelectric Properties of Nanostructured versus Crystalline SiGe," Green Technologies Conference, 2012 IEEE , vol., no., pp.1,4, 19-20 April 2012 doi: 10.1109/GREEN.2012.6200959.